

2011

An elasto-plastic model to describe the undrained cyclic behavior of saturated sand with initial static shear

G Chiaro

University of Wollongong, gchiaro@uow.edu.au

L.I.N. De Silva

Univeristy of Moratuwa

T Kiyota

IIS, University of Tokyo, kiyota@iis.u-tokyo.ac.jp

J Koseki

IIS, University of Tokyo, koseki@iis.u-tokyo.ac.jp

Publication Details

Chiaro, G., De Silva, L., Kiyota, T. & Koseki, J. (2011). An elasto-plastic model to describe the undrained cyclic behavior of saturated sand with initial static shear. 5th International Symposium on Deformation Characteristics of Geomaterials- Volume 2 (pp. 1026-1033). Hanrimwon Co., Ltd..

An elasto-plastic model to describe the undrained cyclic behavior of saturated sand with initial static shear

Chiaro, G.

School of Civil, Mining and Environmental Engineering, University of Wollongong, Australia, gabichiaro@yahoo.it

De Silva, L. I. N.

Department of Civil Engineering, University of Moratuwa, Sri Lanka

Kiyota, T. & Koseki, J.

Institute of Industrial Science, University of Tokyo, Japan

Keywords: constitutive model, cyclic loads, sand, static shear, stress-dilatancy behavior, stress-strain relationship

ABSTRACT: With the aim of simulating the behavior of saturated sand with initial static shear (i.e., sloped ground) undergoing undrained cyclic loading, which leads to liquefaction and large cyclic shear strain development, an elasto-plastic constitutive model which can describe both monotonic and cyclic torsional shear behaviors of saturated sand under drained and/or undrained conditions is presented. It can simulate qualitatively the stress-strain relationship and the effective stress path, even after the specimen enters fully liquefied state. To verify its effectiveness, the proposed model is employed to simulate the results of a series of hollow-cylindrical torsional shear tests on loose Toyoura sand specimens with initial static shear stress under stress-reversal and non-reversal loading conditions.

1. INTRODUCTION

In the last few decades, there has been the need to develop efficient and economic countermeasures against liquefaction in order to decrease seismic damage to buildings, infrastructures and lifeline facilities as well as natural and artificial slopes. In order to satisfy such needs, it is definitely required to incorporate a more elaborate constitutive model into numerical codes which can describe the liquefaction behavior of sand during cyclic loading.

The aim of this paper is to propose an elasto-plastic constitutive model which makes it possible to simulate the effects of initial static shear (i.e., slope ground conditions) on the undrained cyclic behavior of saturated sand, which leads to liquefaction-induced failure of natural and artificial slopes and consequent large shear strain development.

The constitutive model presented herein consists of an improvement of the one developed at the Institute of Industrial Science (IIS), University of Tokyo, by De Silva and Koseki (2011). To simulate drained and undrained large cyclic behavior of sand, the proposed model requires accurate evaluation of the irreversible strain component. In doing so, the quasi-elastic constitutive model, named IIS model (HongNam and

Koseki, 2005), was used to evaluate the elastic shear strain component. Consequently, in analyzing the hollow cylindrical torsional shear test data, the plastic shear strain components were obtained by subtracting from the measured total shear strain component the elastic one. The presence of initial static shear stress was introduced in the model by means of a monotonic drained shear loading path before the undrained one. The two-phase (drained followed by undrained) monotonic loading behavior which is defined in terms of shear stress vs. plastic shear strain relationship (i.e., skeleton curve) was simulated by employing the Generalized Hyperbolic Equation (GHE) model proposed by Tatsuoka and Shibuya (1992). Based on the experimentally obtained skeleton curves, the undrained cyclic shear loading behavior was modeled by using the extended Masing's rules while considering: (a) rearrangement of particles during cyclic loading (drag effect; Tatsuoka et al., 2003); (b) damage of plastic shear modulus at large level of shear stress (De Silva and Koseki, 2011); and (c) hardening of the material during cyclic loading (De Silva and Koseki, 2011). In addition, in modeling the undrained cyclic shear behavior, it was assumed that the total volumetric strain increment during the undrained loading, which consists of dilatancy and consolidation/swelling components, is equal to zero. An empirical four-phase stress-dilatancy relationship, which varies with the amount of damage to

the plastic shear modulus of the material (De Silva and Koseki, 2011), was employed to model the accumulation of volumetric strain increment due to dilatancy and the generation of pore water pressure during the undrained cyclic torsional shear loading. An anisotropic over-consolidation boundary surface was proposed to introduce the combined effects of over-consolidation and initial static shear into the model.

Applicability of the proposed model was verified by simulating the experimental results that were conducted by Chiaro et al. (2011) in order to study the effect of initial static shear stress on the undrained cyclic behavior of saturated Toyoura sand.

2. MODELING OF CYCLIC STRESS-STRAIN BEHAVIOR OF SAND WITH STATIC SHEAR

2.1 Modeling of two-phase skeleton curve by GHE

Monotonic stress-strain relationship (i.e., skeleton curve) of sand subjected to torsional shear loading can be modeled by using the GHE (Tatsuoka and Shibuya, 1992), as described by Eq. (1):

$$Y = \frac{X}{\frac{1}{C_1(X)} + \frac{X}{C_2(X)}} \quad (1)$$

where X and Y are the normalized plastic shear strain and the shear stress parameters, respectively. $C_1(X)$ and $C_2(X)$ are functions of strain:

$$C_1(X) = \frac{C_1(0) + C_1(\infty)}{2} + \frac{C_1(0) - C_1(\infty)}{2} \cos \left\{ \pi / \left(\left| \frac{\alpha'}{X} \right|^{m_t} + 1 \right) \right\} \quad (2)$$

$$C_2(X) = \frac{C_2(0) + C_2(\infty)}{2} + \frac{C_2(0) - C_2(\infty)}{2} \cos \left\{ \pi / \left(\left| \frac{\beta'}{X} \right|^{n_t} + 1 \right) \right\} \quad (3)$$

All the coefficients in Eqs. (2) and (3) can be determined by fitting the experimental data plotted in terms of Y/X vs. X relationship. Note that, $C_1(X=0)$ is the initial plastic shear modulus, while $C_2(X=\infty)$ represents the normalized peak strength of the material.

In this paper, X and Y were defined as follows:

$$X = \gamma^p / \gamma^{ref} \quad (4)$$

$$Y = \frac{(\tau / p')}{(\tau / p')_{\max}} \quad (5)$$

$$\gamma^{ref} = \frac{(\tau / p')_{\max}}{(G_0 / p_0')} \quad (6)$$

where γ^p = plastic shear strain; τ = shear stress; p' = current effective mean principal stress; p_0' = initial effective mean principal stress (= 100 kPa); $(\tau / p')_{\max}$ = peak stress in the plot τ / p' vs. γ^p ; G_0 = initial shear modulus (= 80 MPa).

The plastic shear strain increment ($d\gamma^p$) was evaluated by subtracting from the total shear strain increment ($d\gamma^t$) the elastic one ($d\gamma^e$):

$$d\gamma^p = d\gamma^t - d\gamma^e \quad (7)$$

The elastic component ($d\gamma^e$) was calculated by Eqs. (8) and (9), as formulated in the recently developed quasi-elastic constitutive model (IIS model) proposed by HongNam and Koseki (2005):

$$d\gamma^e = d\tau / G \quad (8)$$

$$G = \frac{f(e)}{f(e_0)} \frac{G_0}{\sigma_0'^n} (\sigma_z' \sigma_r')^{n/2} \quad (9)$$

where G = shear modulus; $f(e) = (2.17 - e)^2 / (1 + e)$, (Hardin and Richart, 1963); $f(e_0)$ = initial void ratio function at $\sigma_z' = \sigma_r' = \sigma_\theta' = 100$ kPa; G_0 = initial shear modulus (= 80 MPa); σ_0' = reference isotropic shear stress (= 100 kPa); σ_z' and σ_r' = vertical and radial effective stress, respectively; and n = material parameter (= 0.508).

In this study, for each test both drained and undrained torsional shear loadings were applied while keeping the specimen height constant. In fact, a specific amount of initial static shear was achieved by applying monotonic drained torsional shear loading; subsequently, the cyclic behavior of sand with static shear was investigated under undrained condition. As shown in Fig. 1, comparison of X - Y relationships from drained and undrained tests revealed a similar behavior of loose sand specimens at the early stage of shearing (i.e., $Y < 0.38$). In view of this consideration and to maintain the continuity of strain development during the change of loading from drained to undrained, it was attempted to model the entire two-phase monotonic loading curve by employing a single set of GHE parameters (Table 1). Typical simulation results of two-phase skeleton curve are shown in Fig. 2.

Table 1. GHE parameters obtained from undrained monotonic shear tests on loose Toyoura sand specimen ($e = 0.828$).

| $C_1(0)$ | $C_1(\infty)$ | $C_2(0)$ | $C_2(\infty)$ |
|----------|---------------|-----------|---------------|
| 35 | 0.123 | 0.102 | 1.2 |
| m_t | n_t | α' | β' |
| 0.43 | 0.43 | 0.00501 | 0.92726 |

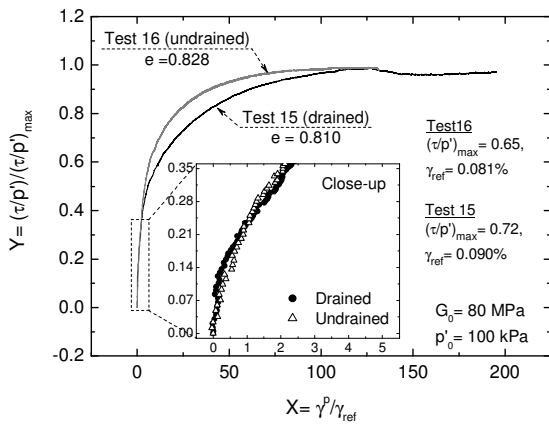


Figure 1. Comparison of X-Y relationships for drained and undrained tests on loose Toyoura sand.

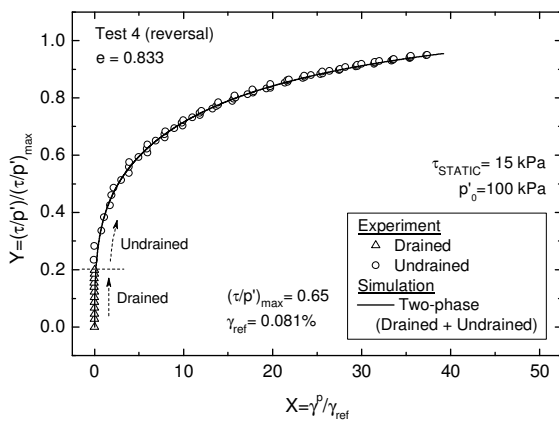


Figure 2. Typical simulation results of a two-phase skeleton curve.

2.2 Modeling of subsequent cyclic loading curves

Cyclic behavior of soil can be modeled by employing the well-known 2nd Masing's rule. However, due to rearrangement of particles, soil behavior does not necessarily follow the original Masing's rule during cyclic loadings (Tatsuoka et al., 1997). This feature can be taken into account by dragging the corresponding skeleton curve in the opposite direction by an amount β while applying the Masing's rule (Masuda et al., 1999; Tatsuoka et al., 2003). In this study the following drag function proposed by HongNam (2004) was used:

$$\beta = \frac{X'}{1 + \frac{X'}{D_1 + D_2}} \quad (10)$$

where D_1 = maximum amount of drag; D_2 = fitting parameter, which is equivalent to the initial gradient of the drag function; and $X' = \Sigma \Delta X$, where ΔX denotes the increment of normalized plastic shear strain.

De Silva and Koseki (2011) introduced two conceptual factors which take into account the damage (D) of

plastic shear modulus at large stress level and the hardening (S) of the material during cyclic loading:

$$D = \frac{\{1 + \exp(-0.8)\}(1 - D_{ult})}{1 + \exp\left\{\left(\Sigma |\Delta \gamma^p|_p\right) - 0.8\right\}} + D_{ult} \quad (11)$$

where D_{ult} = minimum value of D ; $\Sigma |\Delta \gamma^p|_p$ = total plastic shear strain accumulated between the current and the previous turning points;

$$S = 1 + \frac{(\Sigma |\Delta X|)_{up \text{ to current turning point}}}{D_2 + \frac{(\Sigma |\Delta X|)_{up \text{ to current turning point}}}{D_1}} \frac{D_1}{S_{ult} - 1} \quad (12)$$

where S_{ult} = maximum value of S after applying an infinite number of cycles; D_1 and D_2 are the same parameters used in the drag function.

After introducing drag, damage and hardening effects, the skeleton curve during cyclic loading can be modeled as follows:

$$Y = \frac{(X - \beta)}{\frac{1}{C_1(X - \beta) \times D} + \frac{|X - \beta|}{C_2(X - \beta) \times S}} \quad (13)$$

Drag, damage and hardening parameters employed in this study for loose Toyoura sand under constant amplitude cyclic shear loading are listed in Table 2.

Table 2. Drag, damage and hardening parameters.

| D_1 | D_2 | D_{ult} | S_{ult} |
|-------|-------|-----------|-----------|
| 0.25 | 12 | 0.6 | 1.05 |

3. MODELING OF UNDRAINED CYCLIC BEHAVIOR OF SAND WITH STATIC SHEAR

3.1 Stress-dilatancy relationships

Volume change in drained shear, which can be considered as a mirror image of pore water pressure build-up during undrained shear, is one of the key parameters that affect the behavior of sand under cyclic loading. Change of volumetric strain in different stage of loading can be described by the stress-dilatancy relationship, which relates the ratio of plastic strain increments ($-d\epsilon_{vol}^p/d\gamma_{vol}^p$) to the stress ratio (τ/p') (Shahnazari and Towhata, 1992; among others). It should be noted that, the theoretical stress-dilatancy relations, such as Rowe's equations (Rowe, 1962), are derived only for either triaxial ($d\epsilon_2 = d\epsilon_3$ or $d\epsilon_2 = d\epsilon_1$) or simple shear ($d\epsilon_2 = 0$) loading conditions. Therefore they are not directly applicable to the case of torsional shear loading. However, the results from cyclic torsional shear tests suggest that unique relationships between

$-d\varepsilon_{vol}^p/d\gamma^p$ and τ/p' exist either for loading ($d\gamma^p > 0$) and unloading ($d\gamma^p < 0$) conditions (Pradhan et al., 1989). De Silva (2008) proposed an empirical bi-linear stress-dilatancy relationship for cyclic torsional shear loading which is linked with the damage (D) of plastic shear modulus as shown in Eq. (14):

$$\frac{\tau}{p'} = R_k D \left(-\frac{d\varepsilon_{vol}^p}{d\gamma^p} \right) \pm \frac{C}{D} \quad (14)$$

where R_k and C are the gradient and the intercept of the linear stress-dilatancy relationship, respectively; and D is the same as the damage factor in Eq. (11).

During cyclic loadings, the effective mean stress (p') decreases with number of cycles and it can be associated with two potential mechanisms: (i) the soil is subjected to significant effects of over-consolidation until the stress state exceeds for the first time the phase transformation stress state (Ishihara et al., 1975) (i.e., the first time where the volumetric behavior changes from contractive to dilative, $dp' > 0$); and (ii) soil enters into the stage of cyclic mobility. In particular, the over-consolidation significantly alters the stress-dilatancy behavior of sand during the virgin loading and its effect vanishes with the subsequent cyclic loading. To consider the effect of over-consolidation within a certain boundary, Oka et al. (1999) proposed the following stress-dilatancy equations (after De Silva, 2008):

$$-\frac{d\varepsilon_{vol}^p}{d\gamma^p} = \frac{D_k}{R_k} \left(\frac{\tau}{p'} - \frac{\tau/p' - SSR}{\ln(OCR)} \right) \quad (15)$$

$$D_k = \left[\frac{\tau/p' - SSR}{C \ln(OCR)} \right]^{1.5} \quad (16)$$

$$OCR = p_0'/p' \quad (17)$$

In the current study, a modification of the equations proposed by Oka et al. (1999), which consists of a rotation of over-consolidation boundary surface as schematically illustrated in Fig. 3, was made to account for the combined effects of over-consolidation and initial static shear stress on undrained cyclic torsional shear behavior of sand. To this purpose, the following stress-dilatancy equations were proposed to define an anisotropic over-consolidation boundary surface:

$$-\frac{d\varepsilon_{vol}^p}{d\gamma^p} = \frac{D_k}{R_k} \left(\frac{\tau}{p'} - \frac{\tau/p' - SSR}{\ln(OCR)} \right) \quad (18)$$

$$D_k = \left[\frac{\tau/p' - SSR}{C \ln(OCR)} \right]^{1.5} \quad (19)$$

$$SSR = \tau_{static} / p_0' \quad (20)$$

where τ_{static} = initial static shear stress. Note that, whenever $SSR = 0$ (i.e., $\tau_{static} = 0$), Eqs. (18) and (19) meet Eqs. (15) and (16), respectively.

The proposed anisotropic over-consolidation boundary surface has the same features of the one presented by Oka et al. (1999) for isotropically consolidated sands, in the sense that, it defines the region within which the specimen behaves as less contractive while being affected by over-consolidation. As well, it takes into account the effects of anisotropic consolidation induced by initial static shear stress, following the same principle of the rotation of yield surface in the stress space due to anisotropic consolidation (e.g., Taiebat and Dafalias, 2010).

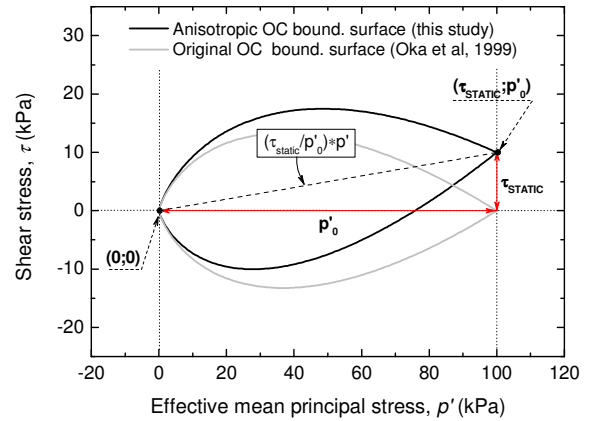


Figure 3. Schematic illustration of original and anisotropic over-consolidation boundary surfaces.

3.2 Four-phase stress-dilatancy model

The stress path during undrained loading was divided into four sections namely: (A) Virgin stress path; (B) Stress path within the limits of phase transformation stress state; (C) Stress path within the limits of over-consolidation boundary surface; and (D) Stress path after exceeding the phase transformation stress state for the first time. The schematic illustration of the four-phase stress-dilatancy relationship is shown in Fig. 4; the coefficients and the equations employed for each phase are listed in Table 3.

Table 3. Four-phase stress-dilatancy parameters.

| Phase | Eq. | R_k | C | D |
|-------|------------|-------|-------|-----|
| A | (14) | 1.7 | 0.595 | 1 |
| B | (14) | 2.2* | 0.45* | 1 |
| C | (18), (19) | 2.2* | 0.45* | 1 |
| D1 | (14), (11) | 2.2* | 0.36* | D |
| D2 | (14), (11) | 0.33* | 0.18* | D |

*After De Silva (2008)

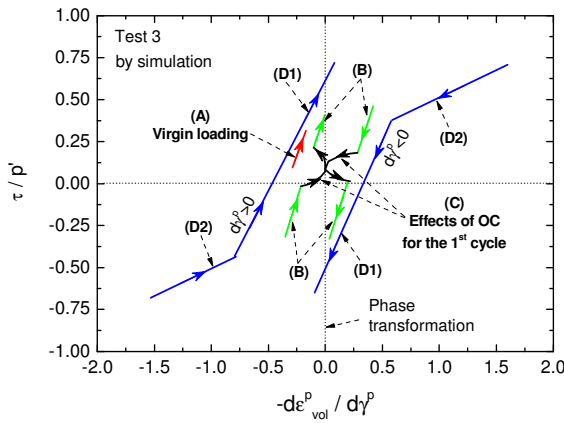


Figure 4. Typical simulation results using the four-phase stress-dilatancy relationship.

3.3 Modeling of pore water pressure generation

In modeling the undrained cyclic shear behavior it was assumed that the total volumetric strain increment ($d\epsilon_{vol}$) during the undrained loading, which consists of dilatancy ($d\epsilon_{vol}^d$) and consolidation/swelling ($d\epsilon_{vol}^c$) components, is equal to zero. In fact, a change of mean effective stress (p') during undrained loading causes the re-compression/swelling of the specimen; on the other hand, a change of shear stress (τ) causes the dilatation of the specimen. Therefore the following equation is valid during undrained cyclic loading:

$$d\epsilon_{vol} = d\epsilon_{vol}^c + d\epsilon_{vol}^d = 0 \quad (21)$$

Experimental evidences suggest that the bulk modulus K ($= dp'/d\epsilon_{vol}^c$) can be expressed as a unique function of the effective mean principal stress (p'):

$$K = \frac{dp'}{d\epsilon_{vol}^c} = K_0 \frac{f(e)}{f(e_0)} \left(\frac{p'}{p_0'} \right)^{m_k} \quad (22)$$

where K_0 = bulk modulus at reference effective mean stress (p_0'); $f(e)$ and $f(e_0)$ = void ratio function at current and reference stress state, respectively; and m_k = coefficient to model the stress-state dependency of K .

Considering that $f(e) = f(e_0)$ in undrained tests, and that the volumetric strain component due to consolidation/swelling is the mirror image of the one due to dilatancy ($d\epsilon_{vol}^c = -d\epsilon_{vol}^d$), the generation of pore water pressure during undrained shearing was evaluated as follows:

$$dp' = K_0 (p'/p_0')^{m_k} (-d\epsilon_{vol}^d) \quad (23)$$

In this, $-d\epsilon_{vol}^d$ was calculated by combining the stress-strain relationship in Eq. (13) with the stress-dilatancy relations in Eq. (14) or Eq. (18). Empirically estimated values of $K_0 = 47$ MPa and $m_k = 0.50$ were used for loose Toyoura sand ($e = 0.828$) at an initial confining stress state of $p_0' = 100$ kPa.

3.4 Modeling of initial static shear effects on the effective stress path

The presence of initial static shear widely affects the monotonic undrained behavior of sand as well as the subsequent cyclic liquefaction behavior (e.g., liquefaction resistance, failure behavior, mode of residual strain development, etc). As well, under the same initial condition of void ratio and effective mean principal stress, the peak undrained strength of sand during monotonic torsional shearing increases with the initial static shear stress (Chiaro, 2010). Herein, the presence of initial static shear stress was simulated by a monotonic drained loading path before the undrained cyclic shearing, with the simplified assumption that no change of p' occurs (i.e., $p' = p_0' = \text{constant}$).

4. COMPARISON BETWEEN EXPERIMENTAL AND SIMULATION RESULTS

To verify the performance of the proposed elasto-plastic constitutive model, the results from a single-element numerical simulation were compared with the experimental data presented by Chiaro et al. (2011).

4.1 Effective stress paths

Typical effective stress paths obtained experimentally and by numerical simulations are shown in Figs. 5 through 7. One can see that, in the case of stress-reversal loading tests, the model is able to simulate the whole liquefaction behavior of sand: specimen first enters into fully liquefied state (i.e., $p' = 0$) and then shows cyclic mobility. On the other hand, simulation results confirm that liquefaction does not take place in the case of non-reversal loading tests in a similar manner as observed in laboratory tests.

Note that, stress-reversal loading tests refers to the case in which during each cycle of loading the combined shear stress value is reversed from positive ($\tau_{max} = \tau_{static} + \tau_{cyclic} > 0$) to negative ($\tau_{min} = \tau_{static} - \tau_{cyclic} < 0$), or vice-versa. On the other hand, non-reversal loading tests refers to the case in which the combined shear stress value is always kept positive ($\tau_{min} > 0$).

4.2 Stress-strain relationships

Typical stress-strain relationships obtained experimentally and by numerical simulations are presented in Figs. 8 through 10. The model is able to simulate qualitatively the experimental data up to a shear strain levels of about $\gamma = 8\%$, before entering a steady state (i.e., no further development of strain during subsequent cycles of loading).

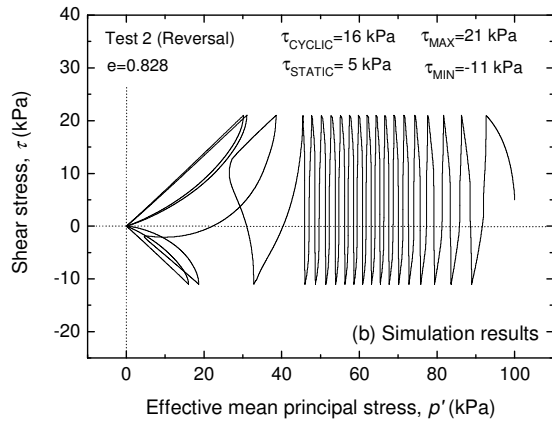
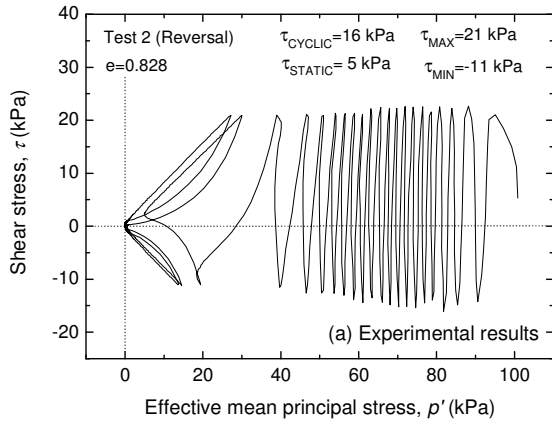


Figure 5. Effective stress paths for Tests 2.

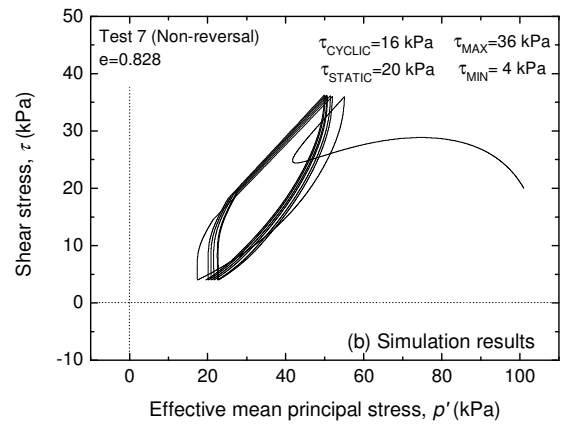
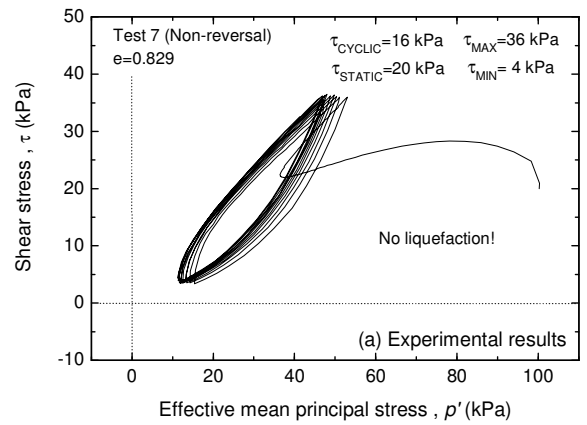


Figure 7. Effective stress paths for Test 7.

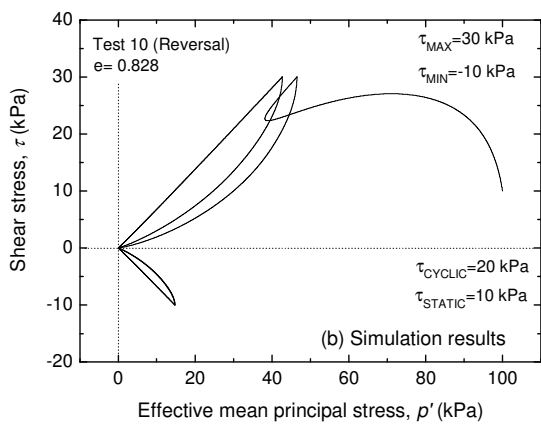
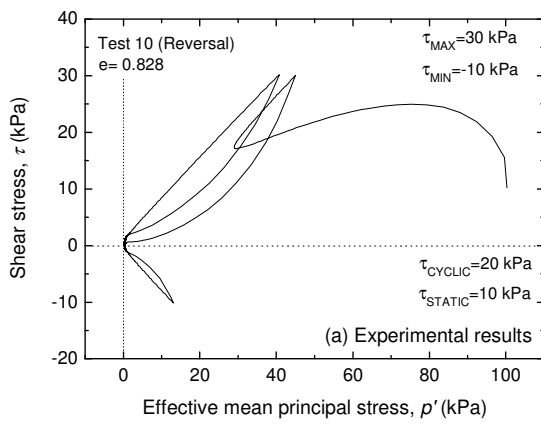


Figure 6. Effective stress paths for Test 10.

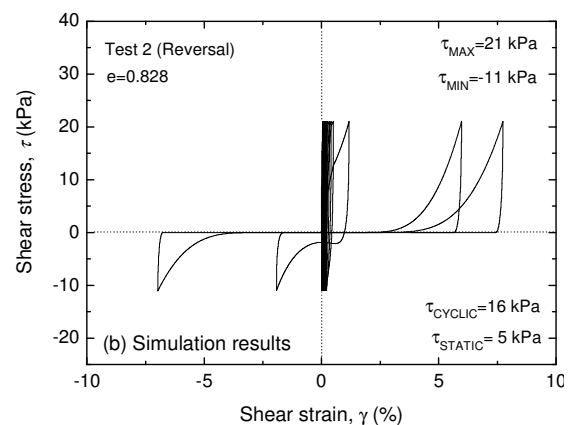
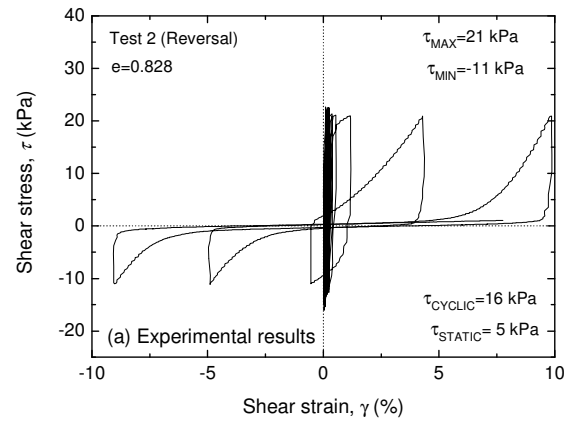


Figure 8. Stress-strain relationships for Test 2.

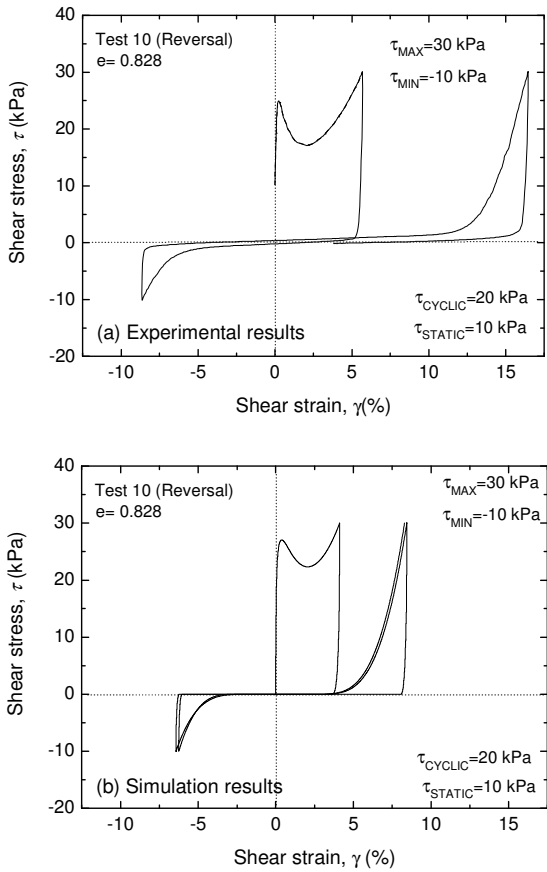


Figure 9. Stress-strain relationships for Test 10.

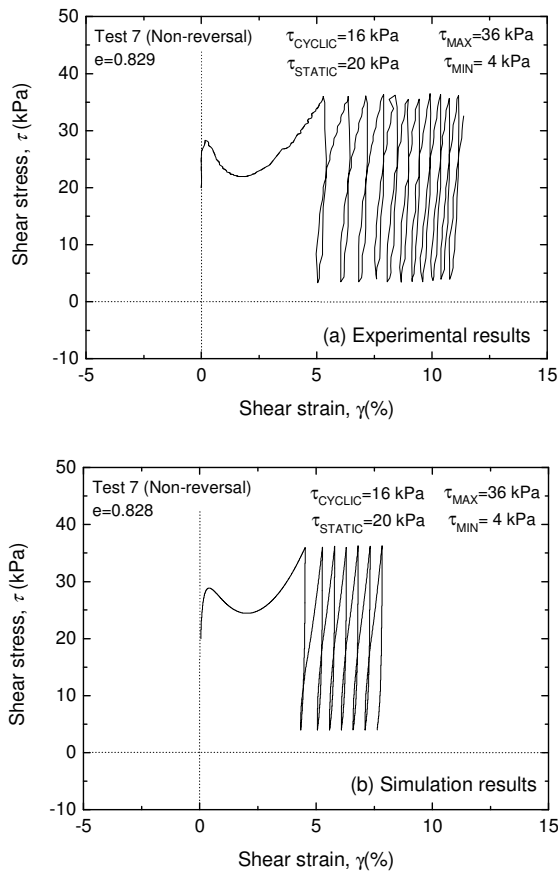


Figure 10. Stress-strain relationships for Test 7.

4.3 Resistance against liquefaction

The resistance against liquefaction (or more strictly, resistance against cyclic shear strain accumulation) was evaluated in terms of number of cycles required to develop a specific amount of single amplitude shear strain of $\gamma_{SA} = 7.5\%$, which would correspond to an axial strain $\epsilon_a = 5\%$ in case of undrained triaxial tests.

Fig. 11 shows the comparison of experimental and simulated liquefaction resistance curves, in terms of relationships between the cyclic stress ratio $CSR (= \tau_{cyclic} / p_0')$ and the number of cycles required to develop $\gamma_{SA} = 7.5\%$.

Note that, the CSR is not a sufficient single parameter to describe the effects of initial static shear on the liquefaction resistance of sand (Chiaro et al., 2011). Therefore, in Fig. 12, the liquefaction resistance curves are also plotted in terms of relationships between the static stress ratio $SSR (= \tau_{static} / p_0')$ and the number of cycles to develop $\gamma_{SA} = 7.5\%$.

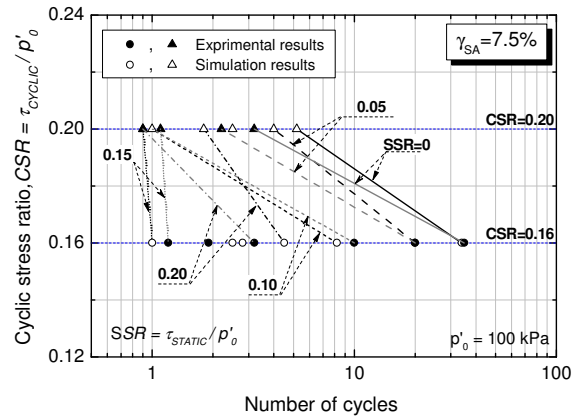


Figure 11. Liquefaction resistance curves defined in terms of cyclic stress ratio (CSR).

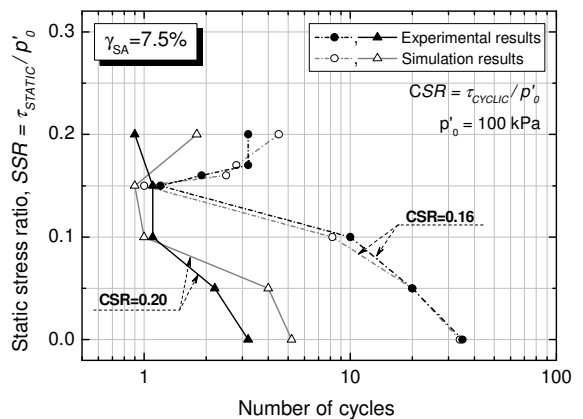


Figure 12. Liquefaction resistance curves defined in terms of static stress ratio (SSR).

Simulation results are consistent with the experimental data. In fact, the resistance against cyclic strain accumulation can either decrease or increase depending on the level of initial static shear and the amplitude of cyclic shear stress in a similar way as observed in laboratory tests.

5. CONCLUSIONS

A cyclic elasto-plastic constitutive model is proposed to simulate the undrained cyclic torsional shear behavior of sand with initial static shear (i.e., sloping ground conditions), which leads to liquefaction and/or large cyclic shear strain development.

The following characteristics are taken into account in the proposed model: (a) the presence of initial static shear stress is introduced by means of a monotonic drained shear loading path before the undrained one; (b) the two-phase skeleton curve (drained followed by undrained) is simulated by employing the GHE model; (c) the subsequent cyclic stress-strain behavior is modeled by using the extended Masing's rules while considering the rearrangement of particles during cyclic loading, the damage of plastic shear modulus at large level of shear stress and the hardening of the material during cyclic loading; (d) the undrained cyclic shear behavior is modeled under the assumption that the total volumetric strain increment during the undrained loading is equal to zero; (e) an empirical four-phase stress-dilatancy relationship, which varies with the amount of damage to the plastic shear modulus of the material, is employed to model the accumulation of volumetric strain increment due to dilatancy and the generation of pore water pressure during the undrained cyclic shear loading; and (f) an anisotropic over-consolidation boundary surface is employed to account for the combined effects of over-consolidation and initial static shear stress.

To verify the performance of the proposed elasto-plastic constitutive model, the simulated results are compared with the experimental data. The model has been found to be capable of reproducing all the features of the undrained cyclic torsional shear behavior of Toyoura sand specimens subjected to initial static shear stress, which are evaluated in terms of effective stress path, stress-strain relationship and liquefaction resistance curves.

The authors recognize limitation of the proposed model in dealing with stress-level and density dependency due to the use of an extensive number of parameters for a single soil type. In fact, for the same sand these parameters have to be calibrated separately if variation of initial relative density and confining pressure are concerned.

REFERENCES

- Chiaro, G. (2010). "Deformation properties of sand with initial static shear in undrained cyclic torsional shear tests and their modeling", PhD Thesis, Dept. of Civil Eng., University of Tokyo, Japan.
- Chiaro, G., Sato, T., Kiyota, T. and Koseki, J. (2011). "Effect of initial static shear stress on the undrained cyclic behavior of saturated sand by torsional shear loading", Proc. of 5th Int. Conf. on Earthquake Geotechnical Engineering, Santiago, Chile, CD-ROM, Paper-ID: EFFCH.
- De Silva, L. I. N. (2008). "Deformation characteristics of sand subjected to cyclic drained and undrained torsional loadings and their modeling", PhD Thesis, Dept. of Civil Eng., University of Tokyo, Japan.
- De Silva, L. I. N. and Koseki, J. (2011). "Modeling of drained and undrained cyclic shear behavior of sand", Proc. of 14th Asian Regional Conf. on SMGE, Hong Kong, (to appear).
- Hardin, B. O. and Richart Jr., F. E. (1963). "Elastic wave velocities in granular soils", Journal of Soil Mechanics and Foundation Division, ASCE, 89 (SM1), 33-65.
- HongNam, N. (2004): "Locally measured deformation properties of Toyoura sand in cyclic and torsional loadings and their modeling", PhD Thesis, Dept. of Civil Eng., University of Tokyo, Japan.
- HongNam, N. and Koseki, J. (2005). "Quasi-elastic deformation properties of Toyoura sand in cyclic triaxial and torsional loadings", Soils and Found., 45 (5), 19-38.
- Ishihara, K., Tatsuoka, F., and Yasuda, S. (1975). "Undrained deformation and liquefaction of sand under cyclic stresses", Soils and Foundations, 15 (1), 29-44.
- Masuda, T., Tatsuoka, F., Yamada, S. and Sato, T. (1999). "Stress-strain behavior of sand in plane strain compression, extension and cyclic loading tests", Soils and Foundations, 39 (5), 31-45.
- Oka, F., Yashima, A., Tateishi, Y., Taguchi, Y. and Yamashita, S. (1999). "A cyclic elasto-plastic constitutive model for sand considering a plastic-strain dependence of the shear modulus", Geotechnique, 49 (5), 661-680.
- Pradhan, T. B. S., Tatsuoka, F. and Sato, Y. (1989). "Experimental stress-dilatancy relations of sand subjected to cyclic loading, Soils and Foundations, 29 (1), 45-64.
- Rowe, P. W. (1962). "The stress-dilatancy relation for static equilibrium of an assembly of particle in contact", Proc. Roy. Soc. London, Series A, 269, 500-527.
- Shahnazari, H. and Towhata, I. (2002). "Torsion shear tests on cyclic stress-dilatancy relationship of sand", Soils and Foundations, 42 (1), 105-119.
- Taiebat, M. and Dafalias, Y. F. (2010). "Simple yield surface expression appropriate for soil plasticity", International Journal of Geomechanics, ASCE, 10 (4), 161-169.
- Tatsuoka, F., Jardine, R. J., Lo Presti, D., Di Benedetto, H. and Kodata, T. (1997). "Characterizing the pre-failure deformation properties of geomaterials, Theme Lecture", Proc. of 14th ICSMFE, Hamburg, Germany, 4, 2129-2164.
- Tatsuoka, F., Masuda, T., Siddiquee, M. S. A. and Koseki, J. (2003). "Modeling the stress-strain relations of sand in cyclic plane strain loading", Journal of Geotechnical and Geoenvironmental Engineering, ASCE, 129 (6), 450-467.
- Tatsuoka, F. and Shibuya, S. (1992). "Deformation characteristics of soil and rocks from field and laboratory tests", Keynote Lecture, 9th Asian Regional Conf. on SMFE, Bangkok, Thailand, 2, 101-170.